International Journal for Housing Science and Its Applications
Publish August 3, 2025. Volume 46, Issue 3 Pages 827-842

https://doi.org/10.70517/ijhsa46362

Research on the construction of intelligent management system for solar photovoltaic-photothermal integrated building supported by Internet of Things based on graph theory algorithm

Hongzhi Wang[1,*], Yunfang Wang[1], Zihao Zhao[1], Jian Pi[1] and Ze Xu[1]
[1] HCIG Xiongan Construction Development Co., Ltd., Xiongan, Hebei, 070001, China
Corresponding authors: (e-mail: wanghongzhi_1970@126.com).

Abstract In this paper, in the planning stage of BIPVT building, the influence of light changes on the temperature of PV panels is considered, and the maximum light radiation of PV panels with different tilt angles is set to determine the optimal installation tilt angle. The photovoltaic part, light part, and photovoltaic photothermal integrated water circulation system are designed in stages. Introduce IoT technology into the BIPVT building, connect the BIPVT building to the Home Assistant system, and design the water circulation control system, intelligent control and remote control, NFC automation control, voice control and other control methods. Considering that the long-term operation of the distribution network of the building system leads to the heating of wires and losses, the Kruskal algorithm is used to solve the mathematical model with the minimization of line losses as the objective function and the improvement of voltage quality as the goal. In the empirical analysis, after the reconfiguration of the distribution network by Kruskal algorithm, the node voltage is increased by 1.25% and the loss is reduced by 15.30%, which proves that the Kruskal algorithm can effectively reduce the loss of the distribution network of the building system and improve the node voltage.In the characterization and testing of the BIPV/T building intelligent system, it is found that the BIPV/T building intelligent system based on the Internet of Things (IoT) is able to effectively improve the indoor thermal environment.

Index Terms BIPVT, Kruskal algorithm, Home Assistant system, node voltage

I. Introduction

In traditional building energy systems, solar photovoltaic (PV) power generation and solar hot water (SW) systems are usually operated independently, lacking effective coordination and integration [1], [2]. The introduction of solar photovoltaic photo-thermal integration (BIPVT) allows these energy sources to be integrated with each other to jointly satisfy the building heat load demand, thus improving energy utilization efficiency and energy conservation and environmental protection [3], [4]. The utilization of solar energy can be divided into photovoltaic (PV) and photo-thermal (PV/T) integration technology is to combine PV and photo-thermal organically, so as to realize the efficient utilization of solar energy [5]. A study by Sultan and Efzan showed that the energy utilization efficiency of solar PV/T system is above 70%, and compared to the single photovoltaic and photo-thermal, in the unit area it can generating more energy, the combined energy efficiency of solar energy is high [6]. Since Kern Jr and Russell first proposed the idea of PV/T in 1978, and developed a new type of flat plate PV/T collector, which realized the integrated utilization of photovoltaic and solar thermal [7]. Subsequently, more and more scholars around the world joined in the research of integrated PV/T technology.Abakam et al. introduced translucent PV into the PV/T collector, constructed a new PV/T system, and simulated the thermal and electrical efficiencies of the PV/T accordingly [8]. Cao et al. pointed out that the PV/T technology can generate both electrical and thermal energy, and that the PV/T integrated building have good potential for controlling indoor air temperature, humidity and air quality [9]. Yao et al. proposed an integrated PCM thermal storage solar PV/T heat pump system for high latitudes, which was found to be a solution to the residential heating problem affected by multiple environmental factors through simulations [10]. Bisengimana et al. investigated different sizes of PV/T systems for energy coverage, explored the power demand of heating and cooling heat pump systems for residential buildings through optimal strategies, and analyzed the economic benefits of PV/T technology in this context [11]. Behzadi and Arabkoohsar proposed a smart building energy system it combines solar photovoltaic thermal (PVT) panels with thermal storage tanks that do not require any batteries to meet the building part of the heat and power demand with high economic efficiency [12]. Therefore, it is of great significance to study in depth the intelligent management of solar photovoltaic photo-thermal integrated buildings.

Internet of Things (IoT) technology is an emerging network technology that utilizes devices to interconnect real-world objects with the Internet to build a tripartite integrated system of users, networks, and devices to achieve information transfer and processing [13]-[15]. The design and construction of smart buildings can also be realized when the building is used as a platform to integrate smart home IoT, cloud computing, intelligent control and other technologies [16]. Tushar et al. proposed an IoT combined with machine learning techniques used to detect building occupancy in order to reduce the energy consumption and cost of building managers [17]. Essa et al. investigated an approach that combines IoT and Artificial Intelligence (AI) techniques for building management system (BMS) to achieve intelligent monitoring, control and management of building energy consumption in educational laboratories [18]. Uzair et al. constructed a low-cost building management system based on IoT technology that provides comprehensive monitoring, control and automation of various environmental and electrical parameters to improve the energy efficiency and safety of buildings [19]. Minoli et al. concluded that IoT based technology can fulfill the smart building needs including comfort, usability etc., security and energy management aspects [20]. Through the relevant research of the above scholars, it is found that the combination of IoT and buildings can realize the intelligent design and management of buildings [21]. For BIPVT buildings, if IoT technology is integrated into BIPVT buildings, parameters such as the power generation efficiency of PV/T modules, the amount of solar radiation received by the modules, the ambient temperature, the temperature of the collector tank, and the surface temperature of the modules can be realized for real-time monitoring and intelligent management [22]-[25]. Intelligent control of the equipment inside the BIPVT building can also be realized through the corresponding design [26].

In this paper, the photovoltaic solar thermal building integration is designed. First, the solar insolation situation is analyzed, including the analysis and design of the shadow shading situation and the determination of the optimal installation inclination angle. Subsequently, the photovoltaic and photothermal parts were designed separately, and the photovoltaic photothermal integrated water circulation system was designed. The designed PV photovoltaic and solar thermal building integrated system is built on Home Assistant system, and various control methods such as water circulation control system, intelligent control and remote control, and NFC automation control are designed. Take advantage of the Kruskal algorithm in the graph theory algorithm to reconstruct the building distribution network. Examples are given to analyze the role of Kruskal algorithm in reconfiguring the distribution network of the building system, and to analyze the operation of the photovoltaic and solar thermal building integrated intelligent system.

II. BIPV/T intelligent system design

II. A. Solar building integration

The main forms of solar building integration include building integrated photovoltaic (BIPV), building integrated solar thermal (BIST) and building integrated photovoltaic/thermal (BIPV/T). Among them, BIPV and BIST systems have been widely used. However, BIPV has problems such as low power generation efficiency, overheating indoors in summer, single function, and light spot pollution, which hinder its large-scale application.BIST, which includes solar water heating technology and passive heating technology, also has problems such as overheating indoors in summer, single function and large temperature fluctuation, low utilization rate throughout the year, and poor indoor comfort.

II. B. Solar photovoltaic solar thermal building integration

Solar photovoltaic solar thermal building integration (BIPV/T) is the integration of solar photovoltaic photovoltaic photovoltaic and thermal comprehensive utilization of technology and buildings, the formation of such as photovoltaic photovoltaic solar thermal roofs, walls, windows, shading facilities, and so on, and in the generation of electricity at the same time, the cooling medium in the system to take away the heat of the batteries to be utilized [27], [28]. It is an important way to realize the efficient use of solar energy by simultaneously meeting the user's demand for high-quality electricity and low-quality heat. It is broadly categorized into building integrated photovoltaic air (BIPV/Air) and building integrated photovoltaic water heating (BIPV/Water) systems.

II. B. 1) Building Integrated Photovoltaic/Air (BIPV/Air)

The cooling medium of BIPV/Air is air, which is categorized into active and passive systems. Active systems usually introduce air into the air flow channels on the backside of the PV panels under the action of a fan to lower the operating temperature of the batteries to increase the power generation efficiency, and at the same time recover heat energy for utilization. The noise of the fan in the system is the main problem that hinders its application.

Passive systems, on the other hand, utilize natural convection to deliver hot air into the room or out of the room under the effect of thermosiphonage and through the Trombe wall principle to achieve passive heating or ventilation cooling.

BIPV/Air has the advantages of low cost, maintenance free and no freezing damage.

II. B. 2) Building Integrated Photovoltaic Water Heating (BIPV/Water)

The cooling medium of BIPV/Water is water, which is categorized into natural circulation type and forced circulation type. The natural circulation type places the water tank above the collector and relies on the buoyancy of the water to carry out the heat collection cycle. The forced circulation type is driven by a pump to circulate the water, which absorbs heat energy and cools the battery to improve power generation efficiency.BIPV/Water has the advantages of simple construction, high thermal efficiency, low cost, and easy to integrate with the building.

II. C.Analysis and Design of Integrated Photovoltaic and Solar Thermal Buildings

II. C. 1) Light analysis

(1) Shadow shading analysis

Considering the photovoltaic panels in the actual work by the irradiance, temperature, the shadow of the impact, photoelectric conversion efficiency can only be achieved in the 13% ~ 15% or so, that is, only 13% ~ 15% of the solar energy will be converted into electrical energy, the rest of the energy is converted into the form of heat energy. Photovoltaic arrays in the shadow or mismatch when the output P-V curve will be shown as a multi-peak characteristics, while the component part of the photovoltaic cell is shading warming and cause hot spot effect. To address this problem, this paper solves it by modeling the heat transfer of PV modules in the case of shading.

In the actual working condition, the temperature response of the PV panel is caused by changes in illumination, so the temperature response change is lagging behind the illumination. Set after a certain time after the PV module to reach thermal equilibrium, the one-dimensional steady state heat balance equation of the PV module is:

$$G_{pv} = \frac{P_{mp}}{A_{pv}} + H_{pvg} + H_{pvs} + R_{pvg} + R_{pvs} \tag{1}$$

According to the structure of photovoltaic module, it is generally divided into three layers: front cover glass layer, battery layer and backsheet, and the following equations can be obtained from the conservation of energy in each layer:

$$a_g G + (\frac{\lambda_g}{d_g})(T_{pv} - T_g) = h_{cga}(T_g - T_a) + h_{rgs}(T_g - T_a) \tag{2}$$

$$(\frac{\tau_g \alpha_{pv}}{(1-(1-\alpha_{pv})(1-\tau_g))} - \eta) = (\frac{\lambda_g}{d_g})(T_{pv} - T_g) + (\frac{\lambda_t}{d_t})(T_{pv} - T_t) \tag{3}$$

$$(\frac{\lambda_t}{d_t})(T_{pv} - T_t) = h_{cta}(T_t - T_a) \tag{4}$$

$$\frac{\tau_g \alpha_{pv}}{1-(1-\alpha_{pv})(1-\tau_g)} G + \frac{P_{con}}{A_{cell}} = (\frac{\lambda_g}{d_g})(T_{pv} - T_g) + (\frac{\lambda_t}{d_t})(T_{pv} - T_t) \tag{5}$$

where α is the absorptivity, τ is the reflectivity, and η is the cell efficiency. λ is the thermal conductivity, d is the thickness, h is the heat transfer coefficient, T is the temperature, and P_{con} is the energy consumed by the counter-biased cell.

As an example, if a single cell is shaded in the 1st battery string, and no cell is shaded in the other strings, there should be a reverse bias in the 1st battery wear, and the current I_d flowing through the bypass diode in the equivalent circuit of the shaded cell is negligible. At this time there is:

$$I_{sh} = I - I_{ph,1-1} \tag{6}$$

$$P_{con} = I_{sh}^2 R_{sh} + I^2 R_s = (I - I_{ph,1-1}) R_{sh} + I^2 R_s \tag{7}$$

$$-(I - I_{ph,1-1}) R_{sh} - IR_s + (m-1)[a \ln(\frac{I_{ph} - I}{I_o} + 1) - IR_s] = -V_{bd} \tag{8}$$

From Eq. (8), it can be seen that in the case of reverse bias of the shaded cell, the current I flowing through the string is mainly related to the shunt resistance R_{sh}, the photogenerated current $I_{ph,1-1}$ of the shaded cell, the series resistance R_s, and the number of cells m in the string protected by the bypass diode.

(2) Determination of optimal mounting tilt angle

Photovoltaic panels at different tilt angles, the amount of radiation received is different, the need to determine the optimal installation of photovoltaic panels tilt angle, so as to maximize the amount of annual radiation received. By the following formula can be derived from the tilted surface of the maximum light radiation calculated value. i.e:

$$H_q = H_{bt} + H_{dt} + H_{rt} \tag{9}$$

$$H_{bt} = R_b H_b \tag{10}$$

$$H_{dt} = H_d[\frac{H_b}{H_0}R_0 + 0.5(1-\frac{H_b}{H_0})(1+\cos\alpha)] \tag{11}$$

$$H_{rt} = 0.5\rho H(1-\cos\alpha) \tag{12}$$

$$H_0 = \frac{24}{\pi}I_{sc}[1+0.033cos(\frac{360n}{365})]\times(cos\varphi cos\delta\sinh_\alpha + \frac{2\pi h}{360}sin\varphi\sin\delta) \tag{13}$$

$$R_b = \frac{\cos(\varphi-\alpha)\cos\delta\sinh_\alpha + (\frac{\pi}{180})h_\alpha\sin(\varphi-\alpha)\sin\delta}{\cos\varphi\cos\delta\sinh_\alpha + (\frac{\pi}{180})\sin\varphi\sin\delta} \tag{14}$$

$$\delta = 23.45^\circ \times \sin\left|\frac{2\pi(284+n)}{365}\right| \tag{15}$$

$$h_\alpha = \min\{h_\alpha, \cos^{-1}[-\tan(\varphi-\alpha)\tan\delta]\} \tag{16}$$

$$H_q = H_b R_b + H_d[\frac{H_d}{H_0}R_0 + 0.5(1-\frac{H_d}{H_0})(1+\cos\alpha)] + 0.5dH(1-\cos\alpha) \tag{17}$$

where H_{bt} is the direct solar radiation, H_{dt} is the scattered radiation from the sky, H_{rt} is the reflected radiation from the ground, α is the inclination angle of the panel, and φ is the geographic latitude. The maximum light radiation from the inclined plane can be derived from (9) and (17).

II. C. 2) Photovoltaic section design

Commonly used photovoltaic cells include monocrystalline silicon cells, polycrystalline silicon cells, amorphous silicon cells, CIGS cells.

After comparative analysis, the photovoltaic cell material selection of the current commonly used polycrystalline silicon, its technology is already more mature technology. The PV array generates electrical energy, which goes through a DC/DC boost chopper circuit to track the maximum power point and output a higher voltage, and then goes through an inverter to provide AC power to the building equipment and other loads.

During operation, insufficient light may occur, i.e., the PV power supply is insufficient to supply the equipment with electricity. Let the power used in the building space be p_{use} and the power generated by the PV be p_{pv}, then there is:

When $p_{use} > p_{pv}$, the building space is switched to the grid power supply, and at this time the power generated by the PV system is stored in the battery bank.

When $p_{use} < p_{pv}$, the building space is switched to the PV system for power supply and the excess power generated by the PV system is connected to the grid.

II. C. 3) Design of the photothermal section

Solar collectors are categorized into flat plate type and vacuum tube type in buildings. From the point of view of building integration, at the early stage of design, the photovoltaic solar thermal components are considered as a roof structure to be considered, and the building space should be selected for flat-plate type solar collectors, which have a higher degree of integration, are more resistant to compression than the vacuum tube type, and have a lower maintenance cost.

The operation method adopts photovoltaic control direct forced circulation system. It is the electricity generated by the photovoltaic to control the pump operation, i.e., forced circulation according to the light condition. In light, the photovoltaic panel generates electricity as a DC power source to turn on the pump, and the water enters the photovoltaic panel to start circulation. When there is no light, the photovoltaic panel stops generating electricity, which is equivalent to the power supply being cut off, and the water pump is turned off. Therefore, the value of hot water produced by the photovoltaic system depends on the actual light condition.

II. C. 4) Water Recycling System Program

In order to improve the efficiency of PV, provide part of the low temperature hot water, and reduce the heat generated by the light on the building, a PV photovoltaic-thermal integrated water circulation system is designed. The control principle of the water circulation system is shown in Figure 1. The design principle of the system is water-cooled circulation, which indirectly controls the temperature of the photovoltaic panels by controlling the temperature of the water circulation. The water circulation system includes photovoltaic panels, a water storage tank divided into upper and lower water tanks (with a heat-insulating plate in the middle), PLC, solenoid valves, motorized valves, converters, energy storage originals, temperature sensors and other components. A convection hole is set in the middle of the water storage tank with a heat-insulating plate, which is divided into an upper water tank (storing hot water) and a lower water tank (full of water in the initial state). One end of the solenoid valve 2 is connected to the tap water pipe, and two solenoid valves are used as switches to control the tap water and the lower water tank, and only one motorized valve is used to control the total flow rate, preventing the whole system from operating in a chaotic manner due to the malfunction of the motorized valve.

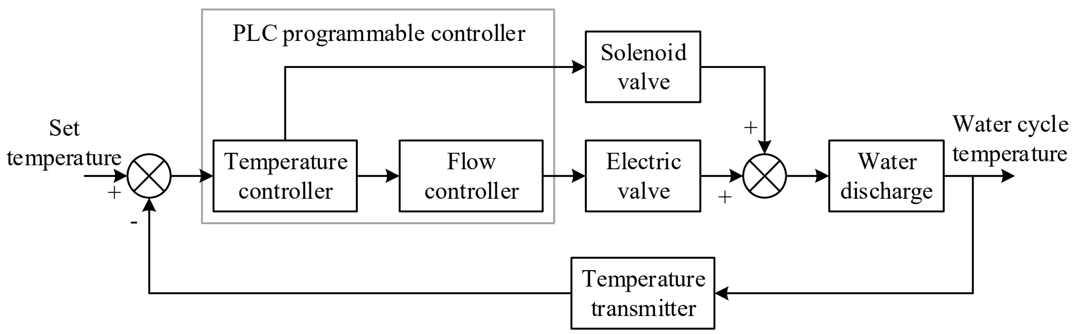

Figure 1: Principle of water circulation system control

II. D.Intelligent management system for BIPV/T buildings based on IoT support

II. D. 1) Home Assistant system

Home Assistant is a free open source software for home automation designed to be a centralized control system for smart home devices, with a primary focus on local control and user privacy. It can be installed on multiple platforms, which include single-board computers, operating systems (e.g., Windows, macOS, Linux), virtual machines, and NAS systems.Home Assistant has the following features:

(1) Support for connecting to and controlling over 1,000 devices: Home Assistant integrates with over 1,000 different devices and services. Once launched, Home Assistant automatically scans the user's network for known devices and allows the user to easily set them up.

(2) Powerful automation features: Once all the devices in the home are integrated, Home Assistant's advanced automation engine can be utilized to implement a variety of automation in the user's home.

(3) Support for expanding the system using add-ons: Home Assistant is not limited to the features it comes with, users can easily install other apps to help them manage their home.

(4) Keeps all smart home data local: Home Assistant stores data locally without the cloud, it communicates with devices locally and will fall back to pulling in data from the cloud if there is no other option. If there is no data stored in the cloud, everything will be handled locally.

(5) Companion mobile apps: The official Home Assistant apps have been developed to quickly control the device and notify the user when something happens in the home. These apps can also be used to send the user's location to the home to use presence detection, which can also be used as part of automation. This data is sent directly to the home with no third party access, thus ensuring user privacy.

(6) Home Energy Management: Home Assistant allows the user to keep track of energy usage in the home through the Home Energy Management feature, which allows optimizing home energy usage and saving energy.

II. D. 2) Design and realization of intelligent control system

For solar photovoltaic photothermal integrated buildings, not only is there a need for control of various types of electrical appliances and equipment, such as solenoid valves, electric valves, home appliances, and control of various switches, but also there are differences in the control methods of different equipment.

In order to achieve the goal of intelligent control of various types of equipment, several control methods such as water cycle control system, intelligent control and remote control, NFC automation control, voice control, etc. are designed based on microcontroller, relay and Home Assistant.

Ⅰ, photovoltaic photothermal (PV/T) water cycle control system design

Photovoltaic (PV/T) water circulation system is an important part of the solar photovoltaic solar thermal integration building, it is due to the existence of the water circulation system, so as to improve the photovoltaic panels of the power generation efficiency, and will be converted into excess heat for the use of the building users of thermal energy.

The solar photovoltaic (PV/T) water circulation control system consists of solar PV modules, hot water storage tanks, temperature sensors, water pumps, water pipes, and valves to form a water circulation system. The control part of the water cycle is based on the STM32 microcontroller and the cloud platform, which controls the valves in the system through relays and allows the measured values of the temperature sensors to be displayed in real time on the terminal device through the Home Assistant.

After successfully connecting to the cloud platform and making relevant initialization settings, the temperature sensor starts to acquire temperature data and sends temperature data to Home Assistant every 10 seconds. When the system meets the on condition, the water circulation system starts working and cycles to determine whether to turn off the system, if so the system will stop working. In addition, the system can also send control instructions to Home Assistant to control the opening and closing of the water circulation system at any time, which realizes the control and management of the operation status of the water circulation system in the cloud.

Ⅱ, intelligent control and remote control

In order to realize intelligent control of all kinds of equipments in PV/T integrated building by using Home Assistant system in smart terminals such as computer, cell phone, iPad, etc., corresponding intelligent design is carried out based on ESPHome in Home Assistant.

ESPHome is the “Build And Deploy” in Home Assistant system, ESPhome supports ESP8266, ESP32 and other devices. ESPhome supports ESP8266, ESP32 and other devices. When all kinds of sensors and relays are connected to the HA system, it only needs to configure the configuration file accordingly to realize the connection between the devices and the HA system; ESPhome realizes the integration through the “auto-discovery” protocol and carries out the whole process of management for compilation and deployment.

Ⅲ, NFC card automation control

Near Field Communication, also known as NFC, is an emerging technology evolved from the integration of interconnection technology, non-contact radio frequency identification (RFID), etc. It is capable of exchanging data in close proximity to support two-way identification and connection, and NFC can be used to realize applications such as mobile payment, access control, and identification through mobile terminals.

The communication mode of NFC has three modes such as point-to-point, read/write mode and card emulation, and the working mode can be divided into passive mode and active mode. With the help of NFC cards, the design and development of smart switches can be carried out, and they can be connected to the Home Assistant system to realize automation control.

After successfully realizing the automation configuration of NFC, the corresponding devices can be triggered by the control buttons on the interface. At the same time, if the NFC-enabled smart terminal devices access Home Assistant, once the NFC card is close to these smart terminal products, it will trigger the corresponding device, thus realizing the goal of NFC control.

Ⅳ, voice control access to Home Assistant system

In the smart home system, voice control refers to the purpose of realizing intelligent control devices through corresponding voice commands. When the Home Assistant system of the solar PV/T integrated building is connected to voice control, all the physical devices in the system can be intelligently controlled by voice commands.

The voice control part is mainly designed and realized through the smart speaker, Bafa MQTT device cloud, and Node-RED. The smart speaker is mainly responsible for receiving and uploading voice control commands. Bafa MQTT Device Cloud is used to create relevant devices, and finally the voice control program is deployed through Node-RED on Home Assistant to achieve the goal of voice control.

V, PV / T building 3D visualization dimming system

For buildings, the lighting system is one of the important components. However, in the building, the distribution of lights is decentralized, and the lights in each room are theoretically independent of each other. In order to control the lights in each room of the BIPVT building more intuitively, the 3D visualization function of Home Assistant is used to visualize the dimming system.

II. D. 3) System Reconfiguration Implementation Based on Graph Theory Algorithms

In this paper, we focus on the mathematical model with line loss minimization as the objective function and voltage quality improvement as the goal.

(1) Model design

Distribution network due to long-term operation, resulting in wire heating loss, in addition to the line loss also includes the transformer work generated by the loss. When carrying out distribution network reconfiguration, network loss generally refers to line loss, so the objective function of minimizing line loss can be expressed as:

$$\min P_L = \sum_{i=1}^{N_s} R_i (P_i^2 + Q_i^2) / U_i^2 \tag{18}$$

where P_L is the objective function and represents the line loss. N_b is the total number of branches in the network, P_i is the active power flowing through the branch b_i and Q_i is the reactive power flowing through the branch b_i, R_t is the branch resistance of the branch b_i and U is the terminal voltage of the branch b_i.

The constraints for distribution network reconfiguration are:

a. The network reconfiguration must satisfy the current equation of the distribution network.

b. Branch current and node voltage constraints. Namely:

$$\begin{cases} I_i \le I_{i,\max} \\ U_{i,\max} \le U_i \le U_{i,\max} \end{cases} (i = 1, 2, ..., n) \tag{19}$$

where n is the number of system nodes. $U_{i,\max}$ is the node U_i allowable voltage upper limit value. $U_{i,\min}$ is the node U_i allowed voltage lower limit value. $I_{i,\max}$ is the upper limit of branch b_i current.

c. The distribution network must satisfy the load demand and have no isolated nodes and no islands.

d. Network topology constraints. The distribution network is planned and designed for closed-loop presentation and open-loop operation, so the reconfigured distribution network operates radially.

The mathematical model with the goal of improving voltage quality, i.e., by changing the operating state of contact switches and sectionalized switches in the reconfiguration, the distribution network presents radial power supply and voltage quality is improved. A loop is formed by closing one contact switch at a time, so the voltage balance index in the loop is defined as VBI_{1-j}:

$$VBL_{i-j} = \max(UN_i, UN_j) / \min(UN_i, UN_j) \tag{20}$$

where $\min(UN_i, UN_j)$ takes the smaller of the two node voltages. $\max(UN_i, UN_j)$ takes the larger of the two node voltages.

So the voltage balance index is used as the objective function in network reconfiguration:

$$f = \min \sum_{i,j<\alpha} VBL_{i-j} \tag{21}$$

The constraints of network reconfiguration are consistent with the constraints of network loss minimization.

In the distribution network network network loss, voltage and balancing load are interrelated, optimizing any one of these indicators can improve the other two indicators, so that the comprehensive performance of the system can be improved, and the desired economic objectives can be obtained. The objective function used in this paper is network loss optimization as the objective. Its expression is:

$$\min f = \sum_{i=1}^{m} \Delta P = \sum_{i=1}^{m} R_i \frac{p_i^2 + Q_i^2}{u_i^2} \tag{22}$$

where m is the total number of branches in the network. P_i is the active power flowing through the branch and Q_i is the reactive power flowing through the branch. R_i is the branch resistance and U_i is the first end voltage of the branch. ΔP is the sum of network losses of all lines in the network.

The objective of the distribution network reconfiguration is to minimize f, the network operates radially, has no isolated nodes, no loops. And the following constraints are satisfied:

$$U_{i,\min} \le U_i \le U_{i,\max} \tag{23}$$

$$I_i \le I_{i,\max} \tag{24}$$

$$S_i \le S_{i,\max} \tag{25}$$

$$\begin{cases} P_i = U_i \sum_{j=1}^{n} U_j (G_{ij} \cos\delta_{ij} + B_{ij} \sin\delta_{ij}) \\ Q_i = U_i \sum_{j=1}^{n} (G_{ij} \sin\delta_{ij} + B_{ij} \cos\delta_{ij}) \end{cases} \tag{26}$$

where $U_{i,\min}$ is the lower voltage limit value of node i. $U_{i,\max}$ is the upper voltage limit value of node i. $I_{i,\max}$ is the maximum value of branch current. $S_{i,\max}$ is the maximum load capacity of distribution transformer or branch i. P_i is the active power injected at node i. Q_i is the reactive power injected at node i, and G_{ij} is the conductance at nodes i,j. B_{ij} is the electricana of node i,j, and δ_{ij} is the voltage phase angle difference of node i,j. n is the total number of nodes in the system, and U_i is the voltage amplitude at node i. U_j is the voltage magnitude of node j.

(2) Weights Acquisition

The key to the calculation of the graph theory algorithm is the determination of the weights, and only by determining the appropriate weights can the graph theory algorithm be utilized to obtain a spanning tree that meets the requirements. In this paper, we take the minimum network loss as the goal for the optimization of distribution network reconfiguration, and the network loss of distribution network can be expressed by Eq. (18), and Eq. (27) is obtained by variation:

$$\min P_L = \sum_{i=1}^{N_t} R_i (P_i^2 + Q_i^2) / U_i^2 = \sum_{i=1}^{N_t} \frac{\Delta U_i^2}{R_i} \tag{27}$$

where P_L is the active loss of the system and ΔU is the voltage drop on the branch.

From the above equation, it can be seen that since the line parameters are constant, when the line voltage drop is smaller the line loss is lower. By using the voltage balance index as the weights, using graph theory algorithm to optimize the distribution grid can get the spanning tree with smaller voltage drop on the branch, and subsequently the active network loss of the system will be reduced. So the inverse of the voltage balance index is utilized as the weights and the weights formula is defined as shown in equation (28):

$$VBL_{i-j} = \min(UN_i, UN_j) / \max(UN_i, UN_j) \tag{28}$$

The determination of the weights requires the data obtained from the tidal flow calculations, and before the tidal flow calculations are performed, the distribution network data first needs to be input to ensure the subsequent calculations.

Before carrying out the graph theory and network optimization algorithm, the actual problem needs to be transformed into the form of a matrix and input into the computer in order to obtain the optimal solution using this optimization method.

(3) System reconfiguration based on Kruskal's algorithm [29], [30]

For a connected assignment graph G, the spanning tree T of G is constructed in the following way: the first edge e_1 with the smallest weight of any edge in G is selected. Select the second edge e_2 with the smallest weight among the remaining edges of G. Select the edge with the smallest weight among the remaining edges of G as the third edge e_3 and do not form a ring with the two previously selected edges, and repeat the above until a spanning tree is produced.

The entire distribution network is represented by a connectivity-assigned graph G, G = (V, E) to represent the set of nodes and edges of a distribution network. The minimum spanning tree T generated satisfies the objective function, which is the optimal solution sought for the distribution network reconfiguration problem. Denoting edges by $l(e)$, the minimum spanning tree of load nodes and root nodes in the distribution network can be expressed as:

$$T = \min \sum_{e_{ij} \in T} l(e_{i,j}) \tag{29}$$

III. System operational characterization and performance testing

III. A. The Role of Graph Theory Algorithms in System Reconfiguration

Taking the typical distribution network of IEEE30 node as an example, distribution network reconfiguration and its implementation strategy to join the optimal network after reactive power optimization are studied and discussed.

Taking the typical distribution network of IEEE30 node as an example, the number of generators of this distribution network is 9, the feeder voltage is 13.12kV, there are 41 branch circuits, 30 nodes, 30 sectionalized switches, 12 contact switches, and the total active load is 2912kW and reactive load is 1304kvar.

After the current calculation of the system with 30 nodes of IEEE by Newton Raphson method, the calculation of distribution network reconfiguration is carried out directly based on the calculated currents. The trend calculation by Newton Raphson algorithm gives the nominal value of each voltage and the corresponding losses of the lines. The lowest voltage node number is 15 and the nominal value of node voltage is 0.924. The line loss is 317.2kW.

The IEEE 30-node distribution system is reconfigured using the Kruskal algorithm mentioned earlier.

After tidal flow calculation by Newton Raphson method, the network loss magnitude of each branch can be obtained as shown in Table 1. The maximum network loss of the distribution system after reconfiguration by Kruskal algorithm arises at (1,5) node number with a value of 64.2kW.

Table 1: The various branch network loss is sorted by size (KW)

Node number	5,3	7,10	9,12	9,13	4,13	10,12	28,23	8,25	14,17
Net loss	0	0	0	0	0	0	0.012	0.024	0.058
Node number	17,19	23,25	24,28	16,20	19,21	10,21	15,24	19,20	29,30
Net loss	0.064	0.075	0.081	0.094	0.1	0.15	0.31	0.32	0.39
Node number	23,24	10,21	23,30	12,19	4,5	6,9	3,4	6,8	5,10
Net loss	0.46	0.54	0.69	0.83	0.92	1.04	1.23	1.37	1.45
Node number	18,19	21,24	26,27	12,17	16,20	6,28	12,24	27,30	10,25
Net loss	2.14	4.36	4.54	5.04	6.72	8.17	9.15	11.0	18.24
Node number	10,23	11,29	6,13	2,7	2,9	2,10	1,4	1,5	/
Net loss	21.45	22.67	28.15	35.72	45.21	55.36	59.3	64.2	/

The initial spanning tree and the initial structure of the network consisting of the minimum branch network loss and the initial structure of the network are obtained for this initial spanning tree with a loss of 315.3 kW, the lowest node voltage is node 21, and the standardized value is chemically 0.9578.

Using Kruskal algorithm, after its objective function for the lowest network loss, iterations are repeated and the smallest tree generated after iterations. The reconstructed network loss is 267.05kW and the minimum voltage of the node is 0.9703 for node 14.

Table 2: Two methods of reconstruction are compared

	Prereconstruction	After the reconstruction of the kruskal algorithm
Open the switch set	1-5	3-5
	2-6	3-9
	2-8	5-6
	5-7	5-7
	6-10	6-10
	9-24	9-21
	10-17	13-18
	21-23	21-23
	23-26	24-29
	15-19	16-24
	16-20	17-25
	24-28	26-30
	28-30	28-30
Network loss(kW)	315.3kW	267.05kW
Minimum node voltage(p.u.)	0.9578	0.9703
Minimum voltage node	21 nodes	14 nodes

Comparison of the reconstruction results of the two methods is shown in Table 2. After Kruskal algorithm for reconfiguration of distribution network in building system, the node voltage is increased by 1.25% and the loss is reduced by 15.30%, this result proves that Kruskal algorithm can be applied in IEEE 30 node distribution network system to improve the power quality and reduce the network loss.

III. B. Characterization of system operation

Based on the design and modeling of the BIPV/T building intelligent management system in the previous section, the BIPV/T intelligent system and the air source heat pump system are simulated, and the operation and system performance of the two systems in different seasons are analyzed in terms of the system loads, the system heating (cooling) effect, and the system energy consumption. The system performance under different system forms is compared in terms of building load and system energy consumption to determine the active and passive effects of PV/T component integration on building energy consumption and the energy efficiency of the BIPV/T intelligent system.

III. B. 1) Comparison of system performance in winter

The daily heat consumption of the building of BIPV/T intelligent system and air source heat pump system in winter is shown in Fig. 2, from which it can be seen that the daily heat consumption of the building of BIPV/T intelligent system is less fluctuating than that of air source heat pump system, and most of the time the daily heat consumption of the building of BIPV/T intelligent system is lower.

It can be seen that the integration of PV/T components in the building can reduce the fluctuation of the building heat load, and most of the time it is beneficial to reduce the building heat load, but part of the time it will increase the building heat load.The actual impact effect of the integration of PV/T components in the building needs to be analyzed for the overall situation in winter.

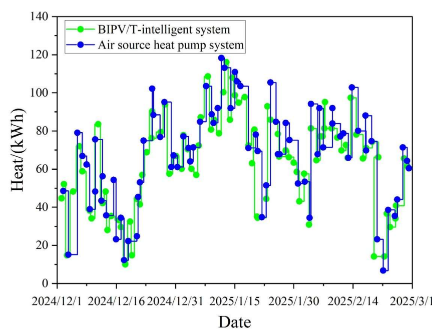

Figure 2: The building day of the winter two systems is summarized

From the meteorological parameters and BIPV/T intelligent system operating temperature to analyze the system impact, in order to analyze the majority of time in winter BIPV/T intelligent system on the effect of the building, this paper selects the average daily outdoor temperature and the average outdoor temperature of the entire heating period is relatively close to the average daily solar radiation is close to the average of solar radiation during the heating period of the typical day to analyze, in this case, select the 20th and 21st of January two days The two days of January 20 and 21 were selected for analysis.

Typical daily meteorological parameters and system operating temperatures in winter are shown in Fig. 3. From the figure, it can be seen that the outer surface temperature of the roof and the PV plate temperature are basically consistent with the trend of the ambient temperature and the intensity of solar radiation. During the daytime when the solar radiation reaches a certain intensity (around 100 W/m^2), the PV panel temperature and the external roof surface temperature are greater than the ambient temperature.

At two o'clock in the afternoon when the solar radiation is the strongest, the PV panel temperature and the external surface temperature of the roof reach the peak, and the temperature of the PV panel almost reaches 50°C. The temperature of the PV/T backsheet does not exceed 40°C, which indicates that the system has a better cooling effect, and most of the heat is taken away by the water flow in the PV/T module. At this time, the temperature of the external surface of the traditional roof is about 28℃, which shows that the integrated PV/T module has a significant impact on the external surface temperature of the roof. During the daytime when solar radiation is strong, the temperature of the roof surface under the integrated PV/T module is about 10℃ higher than that of the traditional roof surface, and the integration of the PV/T module is beneficial to reduce the building heating heat load. At night, when there is no solar radiation, the outside surface temperature of the roof under the integrated PV/T module may be lower than the outside surface temperature of the conventional roof, which will increase the heat load of the building.

Throughout the winter, in most cases, the energy gain from solar radiation absorbed during the day is greater than the increased loss from radiation at night compared to conventional roofs, and the BIPV/T intelligent system can reduce the building heating heat load.

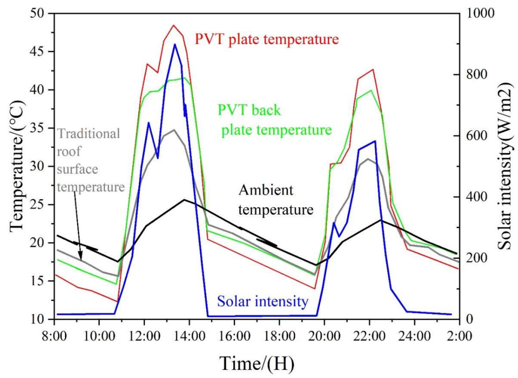

Figure 3: Typical winter meteorological parameters and system operating temperature

III. B. 2) Comparison of system performance during the summer and transition seasons

The daily building cooling loads of BIPV/T smart system and air source heat pump system in summer are shown in Figure 4. From the figure, it can be seen that most of the time BIPV/T smart system building cold load is larger than air source heat pump system building cold load. It can be seen that the integration of PV/T components in the building increases the building cold load most of the time. But part of the time can reduce the building cold load.

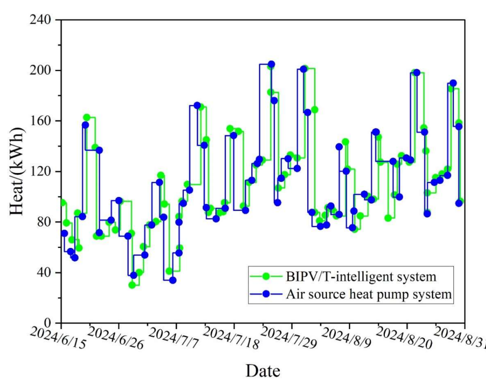

Figure 4: Summer BIPV/T system and air source heat pump system building solar load

III. B. 3) System energy consumption

Comparison of energy consumption of BIPV/T smart system and air source heat pump system in summer and winter is shown in Table 3. The BIPV/T intelligent system in summer and transition season significantly reduces the domestic hot water energy consumption, but increases the cooling energy consumption of the system. The energy consumption of domestic hot water is reduced by 66.27%, cooling energy consumption is increased by 8.8%, and the net power generation of PV/T module (removing the energy consumption of PV/T circulating pump) is 8781.3kWh. Compared with the air source heat pump system, the energy consumption of BIPV/T intelligent system in summer and transitional season is more than 10,000kWh. It can be seen that the energy saving of BIPV/T intelligent system mainly lies in the generation of electricity and the reduction of domestic hot water energy consumption. In the summer, the BIPV/T intelligent system has more than 10,000kWh in the summer and transitional seasons, compared with the BIPV/T intelligent system.

In winter, the BIPV/T intelligent system significantly reduces the energy consumption of building heating and domestic hot water, of which the energy consumption of building heating is reduced by 18.80%, the energy consumption of domestic hot water is reduced by 71.95%, and the net power generation of PV/T module (removing the energy consumption of the PV/T circulating pump) is 2959.3kWh. It can be seen that the energy saving of the

BIPV/T intelligent system in winter mainly lies in the generation of electricity and the reduction of domestic hot water energy consumption. The energy efficiency of the BIPV/T intelligent system in winter is mainly in the reduction of electricity generation and domestic hot water energy consumption, and the reduction of heating energy consumption is limited.

Table 3: The energy consumption comparison of the two systems in summer and winter

Season	Categories	Refrigeration energy consumption (kWh)	Energy consumption in hot water (kWh)	PV/T pump energy consumption (kWh)	PV/T Generating capacity (kWh)	Total
Summer	Air source heat pump system	2855.7	2423.6	2980.2	17894.6	-9635.1
	BIPV/T-intelligent system	3107.1	817.5	2471.9	11253.2	-4856.7
Winter	Air source heat pump system	2302.8	763.9	283.4	3569.4	-6919.5
	BIPV/T-intelligent system	1869.3	214.3	199.0	3158.3	-5440.9

III. C. BIPVT Experimental Room Performance Testing and Analysis

III. C. 1) Design of the actual test program

The purpose of the experimental program test is to quantitatively analyze the performance of the BIPVT experimental room system under the conditions of the meteorological day of the coldest month of winter in a certain place, and here the system performance monitoring platform will be utilized to monitor the performance of the exhibition hall part of the BIPVT experimental room. On this basis, the control group of the actual test program is added, and the performance improvement effect of the indoor thermal environment control strategy based on the BIPVT intelligent system on the BIPVT experimental room is analyzed by means of comparative experiments, including the effect of the improvement of the indoor thermal environment as well as the energy-saving effect of the building.

Based on the hour-by-hour indoor ambient temperature values collected by the performance monitoring platform for each working condition day, a comparison is made with the lower limit value of the tolerance temperature of 13°C and the design heating temperature value of 18°C.

Specifically included:

Working condition day 1, working condition day 2, solar photovoltaic collector system operation mode is carried out in the BIPVT experimental room, and the two corresponding solar photovoltaic collector systems above the exhibition hall are operated, with the temperature start-up threshold value of 18℃.

Work condition day 3, intelligent system control operation mode is carried out in the BIPVT experimental room, and the corresponding southern solar PV collector system above the exhibition hall is running in winter scenario mode.

On Work Condition Day 4, the BIPVT experimental room operates in the air-energy hot-air conditioning mode, and the operating temperature is set at 18℃.

On working condition day 5, the intelligent system control operation mode is carried out in the BIPVT experimental room, and the corresponding solar photovoltaic collector system on the north side above the exhibition hall is running the winter scene mode.

On working condition day 6, the intelligent system control operation mode is carried out in the BIPVT experimental room, and the solar photovoltaic collector system in the north and south corresponding to the exhibition hall runs in the winter scene mode.

III. C. 2) Effectiveness of improvement of indoor thermal environment

(1) Case 1, Case 2

Comparison of various indoor temperatures is shown in Figure 5. The average value of the original indoor temperature is around 6°C. Compared with the original indoor temperature change of the experimental room, after the solar PV collector system is integrated with the building in Case 1 and Case 2, the indoor daytime hour-by-hour temperature is improved compared with the original indoor hour-by-hour temperature.

The average values of indoor temperatures on Case Day 1 and Case Day 2 were about 12.35°C and 10.11°C, respectively. When comparing Condition 1 and Condition 2, the fluctuation of the indoor hour-by-hour temperature curve on Condition 1 was larger, and the indoor temperature was above the "indoor tolerance temperature line" from about 13:00 to 13:30. In Case 2, the fluctuation of the indoor time-by-time temperature curve is smaller, around 10:30 to 12:30, and the heating effect of the solar PV collector system is obvious.

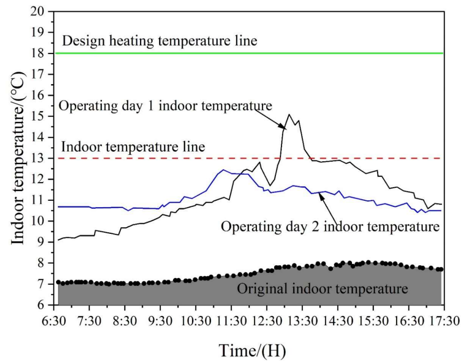

Figure 5: Indoor temperature contrast

(2) Working condition 3

The time-to-time variation of the indoor temperature on Case 3 is shown in Figure 6. All the time periods were above the "indoor tolerance temperature line of 13°C". The time period in which the indoor temperature fell below the design heating temperature line was from about 10:00 to 14:30. Compared with the original indoor temperature profile, the average indoor temperature on condition day 3 was about 10°C or more higher than the original average indoor temperature.

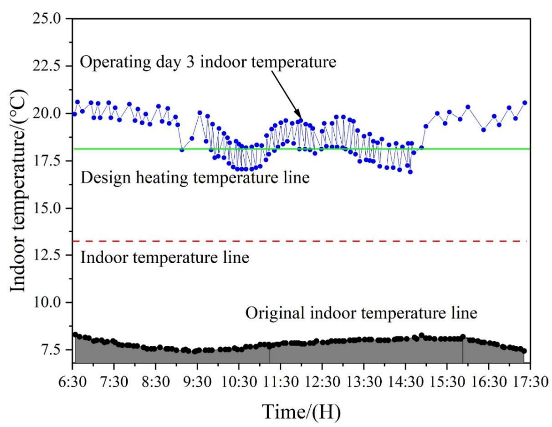

Figure 6: The indoor temperature of the operating day 3 is changed by time

(3) Operating condition 4

The time-by-time curve of the indoor temperature for Case 4 is shown in Fig. 7. Before 8:30 on that day, the indoor temperature was within the "design heating temperature" level line, and after 8:30 the indoor temperature was higher than the "design heating temperature" level line, and maintained at 18.5℃ temperature line up and down, and the overall trend of the temperature curve remained at the same level, in line with the threshold setting for air conditioners in the control strategy. The overall trend of the temperature curve remains at the same level, which is in line with the threshold setting of air conditioning in the control strategy.

(4) Operating condition 5

The time-by-time curve of the indoor temperature for Case 5 is shown in Fig. 8. The overall temperature is above the "tolerable indoor temperature line of 13℃". It fluctuates up and down at the "design heating temperature line of 18°C", and the time period below 18°C is mainly from 9:00 to 15:00. From the analysis, the outdoor meteorological parameters of Case 5 are at a low level, which affects the performance of the solar PV collector system by influencing the impact on the indoor thermal environment.

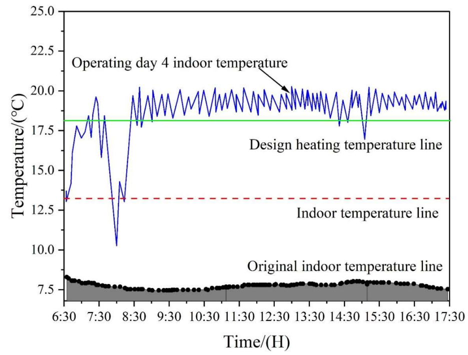

Figure 7: The indoor temperature hour curve of the operating day 4

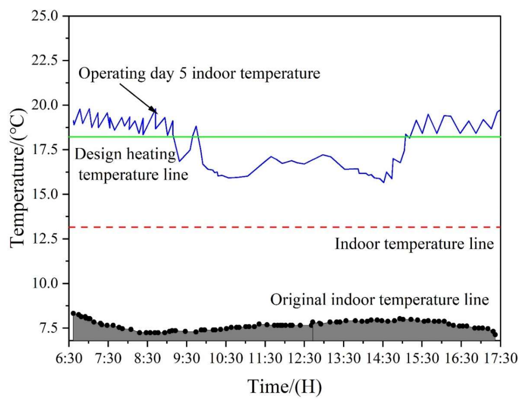

Figure 8: The indoor temperature hour curve of the operating day 5

(5) Case 6

The time-by-time curve of the indoor temperature for Case 6 is shown in Figure 9, which is above the "design heating temperature line". The indoor temperature is higher than that of the air-conditioning system during the intervention time of the solar PV collector system. Compared with the original indoor temperature curve, the average indoor temperature is higher than 10℃.

From the analysis, the working condition day 6 under the dual intelligent system control mode, compared with the working condition days 3 and 5 under the single intelligent system control mode, the dual intelligent system control mode is more effective in improving the indoor thermal environment in the time period from 9:30 to 14:30.

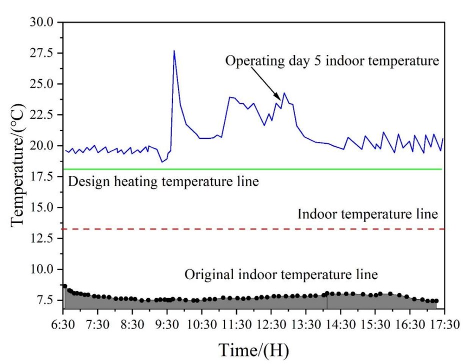

Figure 9: The indoor temperature hour curve of the operating day 6

(6) BIPV/T intelligent system performance results

The building performance results from Case 1 to Case 6 are shown in Table 4, summarizing the cumulative heat consumption saving rate and indoor thermal environment improvement effect data of the building heating season for Case Day 1 and Case Day 6.

From the system supply energy under Case 3, 4 and 6 as the average value of the system performance under the average meteorological conditions of the coldest month, the calculated changes in the building energy consumption show that the total energy consumption savings are over 35% (excluding the energy saving part of the operation of the air conditioner for air energy heat and air conditioning), with the highest saving rate under Case 6.

Table 4: Performance results of the performance of 1 to operating condition

Operating day	Heat collection (kWH) /Calorie consumption	Generating capacity (kWH) /consumption of electricity consumption	Indoor temperature mean(℃)	Tolerance temperature interval number(H)
Condition day 1	152.34/31.5%	150.73/counterbalance	12.35	2
Condition day 2	23.76/5.69%	68.53/counterbalance	10.11	0
Condition day 3	159.86/33.75%	53.4/counterbalance	16.45	6
Condition day 4	3.75/0.12%	80.19/counterbalance	18.5	6
Condition day 5	149.5/32.9%	67.05/counterbalance	17.24	12
Condition day 6	153.6/29.8%	159.31/counterbalance	18.56	12

IV. Conclusion

In this paper, we design and build a BIPV/T building intelligent management system supported by Kruskal algorithm, which is paired with Home Assistant system to realize multi-platform and multi-operation. We analyze the operation characteristics of the BIPV/T building intelligent management system, and test the energy-saving performance of the BIPV/T experimental room controlled by the BIPV/T intelligent system in combination with different working day conditions.

(1) Kruskal algorithm in graph theory algorithm can realize the role of improving node voltage and reducing network loss in the example analysis of building distribution network, and effectively solve the mathematical model set in this paper with line loss minimization as the objective function and improving voltage quality as the goal.

(2) The BIPV/T intelligent system can reduce the energy consumption of domestic hot water by 66.27% and 71.95% in summer and winter, respectively, and the net power generation of PV/T modules (removing the energy consumption of PV/T circulating pumps) is 8781.3kWh and 2959.3kWh, respectively, which can be seen that the energy saving of the BIPV/T intelligent system mainly lies in the generation of electricity and the reduction of domestic hot water consumption, but the reduction of energy consumption is limited in the case of building heating. Energy consumption reduction is limited.

(3) After the application of BIPV/T building intelligent management system, the indoor daytime hourly temperature is improved compared with the original indoor hourly temperature, and all of them show different degrees of heat consumption saving rate.

References

[1] Mahmoud, R., Kamara, J. M., & Burford, N. (2020). Opportunities and limitations of building energy performance simulation tools in the early stages of building design in the UK. Sustainability, 12(22), 9702.

[2] Reynolds, J., Rezgui, Y., & Hippolyte, J. L. (2017). Upscaling energy control from building to districts: Current limitations and future perspectives. Sustainable Cities and Society, 35, 816-829.

[3] Debbarma, M., Sudhakar, K., & Baredar, P. (2017). Comparison of BIPV and BIPVT: A review. Resource-Efficient Technologies, 3(3), 263-271.

[4] Rajoria, C. S., Agrawal, S., Chandra, S., Tiwari, G. N., & Chauhan, D. S. (2016). A Novel investigation of building integrated photovoltaic thermal (BiPVT) system: A comparative study. Solar Energy, 131, 107-118.

[5] Ma, X., Ghosh, A., Cuce, E., & Saboor, S. (2024). Building integrated photovoltaic-thermal systems (BIPVT) and spectral splitting technology: A critical review. Next Sustainability, 4, 100056.

[6] Sultan, S. M., & Efzan, M. E. (2018). Review on recent Photovoltaic/Thermal (PV/T) technology advances and applications. Solar energy, 173, 939-954.

[7] Kern Jr, E. C., & Russell, M. C. (1978). Combined photovoltaic and thermal hybrid collector systems (No. COO-4577-3; CONF-780619-24). Massachusetts Inst. of Tech., Lexington (USA). Lincoln Lab..

[8] Abakam, M., Alkaff, S. A., Go, Y. I., & Venkiteswaran, V. K. (2019). Modelling and performance analysis of a new PVT system, with two semi-transparent PV panels. Process Integration and Optimization for Sustainability, 3, 359-373.

[9] Cao, X., Li, N., Li, Y., Che, L., Yu, B., & Liu, H. (2023). A review of photovoltaic/thermal (PV/T) technology applied in building environment control. Energy and Built Environment.

[10] Yao, J., Xu, H., Dai, Y., & Huang, M. (2020). Performance analysis of solar assisted heat pump coupled with build-in PCM heat storage based on PV/T panel. Solar Energy, 197, 279-291.

[11] Bisengimana, E., Zhou, J., Binama, M., Nyiranzeyimana, G., & Yuan, Y. (2023). Numerical investigation of PVT coverage on an integrated building-solar-heat pump system: Technical and economic study. Solar Energy, 249, 507-520.

[12] Behzadi, A., & Arabkoohsar, A. (2020). Feasibility study of a smart building energy system comprising solar PV/T panels and a heat storage unit. Energy, 210, 118528.

[13] Rose, K., Eldridge, S., & Chapin, L. (2015). The internet of things: An overview. The internet society (ISOC), 80(15), 1-53.

[14] Shah, S. F. A., Iqbal, M., Aziz, Z., Rana, T. A., Khalid, A., Cheah, Y. N., & Arif, M. (2022). The role of machine learning and the internet of things in smart buildings for energy efficiency. Applied Sciences, 12(15), 7882.

[15] Jia, M., Komeily, A., Wang, Y., & Srinivasan, R. S. (2019). Adopting Internet of Things for the development of smart buildings: A review of enabling technologies and applications. Automation in construction, 101, 111-126.

[16] Wei, C., & Li, Y. (2011, September). Design of energy consumption monitoring and energy-saving management system of intelligent building based on the Internet of things. In 2011 international conference on electronics, communications and control (ICECC) (pp. 3650-3652). IEEE.

[17] Tushar, W., Wijerathne, N., Li, W. T., Yuen, C., Poor, H. V., Saha, T. K., & Wood, K. L. (2018). Internet of things for green building management: disruptive innovations through low-cost sensor technology and artificial intelligence. IEEE Signal Processing Magazine, 35(5), 100-110.

[18] Essa, M. E. S. M., El-shafeey, A. M., Omar, A. H., Fathi, A. E., Maref, A. S. A. E., Lotfy, J. V. W., & El-Sayed, M. S. (2023). Reliable integration of neural network and internet of things for forecasting, controlling, and monitoring of experimental building management system. Sustainability, 15(3), 2168.

[19] Uzair, M., Yacoub Al-Kafrawi, S., Manaf Al-Janadi, K., & Abdulrahman Al-Bulushi, I. (2022). A low-cost IoT based buildings management system (BMS) using arduino mega 2560 and raspberry pi 4 for smart monitoring and automation. International journal of electrical and computer engineering systems, 13(3), 219-236.

[20] Minoli, D., Sohraby, K., & Occhiogrosso, B. (2017). IoT considerations, requirements, and architectures for smart buildings—Energy optimization and next-generation building management systems. IEEE Internet of Things Journal, 4(1), 269-283.

[21] Chen, Y., Wang, X., Liu, Z., Cui, J., Osmani, M., & Demian, P. (2023). Exploring building information modeling (bim) and internet of things (iot) integration for sustainable building. Buildings, 13(2), 288.

[22] Gautam, K. R., & Andresen, G. B. (2017). Performance comparison of building-integrated combined photovoltaic thermal solar collectors (BiPVT) with other building-integrated solar technologies. Solar energy, 155, 93-102.

[23] Lamnatou, C., Notton, G., Chemisana, D., & Cristofari, C. (2020). Storage systems for building-integrated photovoltaic (BIPV) and building-integrated photovoltaic/thermal (BIPVT) installations: Environmental profile and other aspects. Science of the Total Environment, 699, 134269.

[24] Yu, J. S., Kim, J. H., & Kim, J. T. (2019). A study on the thermal performance of air-type BIPVT collectors applied to demonstration building. Energies, 12(16), 3120.

[25] Ibrahim, A., Fudholi, A., Sopian, K., Othman, M. Y., & Ruslan, M. H. (2014). Efficiencies and improvement potential of building integrated photovoltaic thermal (BIPVT) system. Energy conversion and management, 77, 527-534.

[26] Fakhabi, M. M., Hamidian, S. M., & Aliehyaei, M. (2024). Exploring the role of the Internet of Things in green buildings. Energy Science & Engineering, 12(9), 3779-3822.

[27] Haotian Yang,Xingjiang Liu,Chaojie Wang,Chao Shen,Rongtao Han,Soteris A. Kalogirou & Julian Wang. (2024). Investigation on the heating performance of a BIPV/T façade coupled with direct-expansion heat pump system in severe cold region. Renewable Energy,232,121065-121065.

[28] Prapavee Karunyasopon,Dong Yoon Park,Duc Minh Le & Seongju Chang. (2024). Performance analysis of transparent BIPV/T double skin façades integrated with the decision-making algorithm for mixed-mode building ventilation. Architectural Engineering and Design Management,20(5),1141-1163.

[29] Ren Liu. (2024). Innovative Research on Synergistic Development of Digital Integrated Media and Visual Design Based on Kruskal Algorithm. Applied Mathematics and Nonlinear Sciences,9(1).

[30] Jingwen Li,Yaodong Han,Qinyi Li & Daizhong Tang. (2024). Optimizing Public Space in High-Rise Residences: A Whole Life Cycle Perspective with Kruskal Algorithm—A Case Study of a Shanghai High-Rise Residential Project. Buildings,14(6),1769-1769.